GRPR versus PSMA: expression profiles during prostate cancer progression demonstrate the added value of GRPR-targeting theranostic approaches

Marjolein Verhoeven[1], Eline A. M. Ruigrok[1], Geert J. L. H. van Leenders[2], Lilian van den Brink[1], Hayri E. Balcioglu[3], Wytske M. van Weerden[4] and Simone U. Dalm[1]*

[1]Department of Radiology & Nuclear Medicine, Erasmus MC, University Medical Center Rotterdam, Rotterdam, Netherlands, [2]Department of Pathology, Erasmus MC Cancer Institute, University Medical Center Rotterdam, Rotterdam, Netherlands, [3]Department of Medical Oncology, Erasmus MC, University Medical Center Rotterdam, Rotterdam, Netherlands, [4]Department of Experimental Urology, Erasmus MC, University Medical Center Rotterdam, Rotterdam, Netherlands

Introduction: Central to targeted radionuclide imaging and therapy of prostate cancer (PCa) are prostate-specific membrane antigen (PSMA)-targeting radiopharmaceuticals. Gastrin-releasing peptide receptor (GRPR) targeting has been proposed as a potential additional approach for PCa theranostics. The aim of this study was to investigate to what extent and at what stage of the disease GRPR-targeting applications can complement PSMA-targeting theranostics in the management of PCa.

Methods: Binding of the GRPR- and PSMA-targeting radiopharmaceuticals [^{177}Lu]Lu-NeoB and [^{177}Lu]Lu-PSMA-617, respectively, was evaluated and compared on tissue sections of 20 benign prostatic hyperplasia (BPH), 16 primary PCa and 17 progressive castration-resistant PCa (CRPC) fresh frozen tissue specimens. Hematoxylin-eosin and alpha-methylacyl-CoA racemase stains were performed to identify regions of prostatic adenocarcinoma and potentially high-grade prostatic intraepithelial neoplasia. For a subset of primary PCa samples, RNA *in situ* hybridization (ISH) was used to identify target mRNA expression in defined tumor regions.

Results: The highest median [^{177}Lu]Lu-NeoB binding was observed in primary PCa samples, while median and overall [^{177}Lu]Lu-PSMA-617 binding was highest in CRPC samples. The highest [^{177}Lu]Lu-NeoB binding was observed in 3/17 CRPC samples of which one sample showed no [^{177}Lu]Lu-PSMA-617 binding. RNA ISH analyses showed a trend between mRNA expression and radiopharmaceutical binding, and confirmed the distinct GRPR and PSMA expression patterns in primary PCa observed with radiopharmaceutical binding.

Conclusion: Our study emphasizes that GRPR-targeting approaches can contribute to improved PCa management and complement currently applied PSMA-targeting strategies in both early and late stage PCa.

1 Introduction

Prostate cancer (PCa) is the second most common male cancer type with 1.4 million new cases and 375.000 deaths worldwide in 2020 (1). In recent years, nuclear medicine has rapidly gained an important status in PCa management. Central to targeted radionuclide imaging and therapy of PCa are prostate-specific membrane antigen (PSMA)-targeting radiopharmaceuticals (2). PSMA is a type II transmembrane glycoprotein that is expressed in normal prostate tissue with significantly increased expression in PCa, especially in advanced stages of the disease (3–6). Following the success of various clinical studies, the radiopharmaceuticals [^{68}Ga]Ga-PSMA-11 and [^{18}F]F-DCFPyL for positron emission tomography (PET) and [^{177}Lu]Lu-PSMA-617 for radionuclide treatment have recently been approved by the FDA and EMA for PCa patients (7–9).

PSMA PET has shown to detect pelvic lymph nodes and metastatic lesions with higher sensitivity and specificity compared to conventional imaging methods such as computed tomography (CT) and bone scintigraphy (10, 11). Regarding treatment with [^{177}Lu]Lu-PSMA-617, impressive results were obtained in PSMA-positive metastatic castration-resistant PCa (mCRPC) patients who received [^{177}Lu]Lu-PSMA-617 plus standard of care versus standard of care treatment alone; with significantly prolonged progression-free survival and overall survival of 8.7 vs. 3.4 months and 15.3 vs. 11.3 months, respectively (12). Importantly, a proportion (<10%) of prostate carcinomas has low PSMA expression and ~30% of mCRPC patients do not respond to treatment with [^{177}Lu]Lu-PSMA-617, when response is defined as any decrease in prostate-specific antigen (PSA) levels (13, 14). Moreover, serious side effects have been frequently reported, such as xerostomia as a consequence of unwanted but specific binding to PSMA in the salivary glands. The impact of xerostomia on patients' quality of life is the main reason for treatment discontinuation, especially when [^{225}Ac]Ac-PSMA-617 is applied (15). All of the above underline the need for new developments with improved efficacy and safety.

The gastrin-releasing peptide receptor (GRPR) is a G-protein coupled receptor that has been investigated as an attractive target for the detection and treatment of several cancer types, including PCa (16). In PCa, overexpression of the GRPR was reported in 63-100% of cases (17). In contrast to PSMA, GRPR overexpression has primarily been associated with low-grade disease (18–22). Initial imaging studies using GRPR-targeting radiopharmaceuticals, such as [^{68}Ga]Ga-RM2, [^{68}Ga]Ga-RM26, [^{68}Ga]Ga-SB3 and [^{68}Ga]Ga-NeoBOMB1/NeoB, have shown promising results in the detection of prostate lesions and lymph node metastases of newly diagnosed and recurrent PCa. While these radiopharmaceuticals have mainly been investigated in exploratory studies, the findings suggest that their use, similar to PSMA targeting, could be superior to conventional imaging (23–27). Following the theranostic approach, clinical studies have been initiated to characterize GRPR ligands coupled to a therapeutic radionuclide (e.g. Lu-177 or Pb-212) in various neoplasms (NCT03872778, NCT05283330) (28).

NeoB, formerly called NeoBOMB1, is a GRPR theranostic agent that has been extensively validated in preclinical and initial clinical studies with promising results (27, 29–31). Although studies with GRPR radiopharmaceuticals, including NeoB, have demonstrated high uptake not only in the tumor, but also in the GRPR-expressing pancreas, multiple studies have shown that the pancreas is not expected to be a dose limiting organ for GRPR-mediated treatment (28, 30, 32). The relatively low estimated absorbed dose by the pancreas is most likely due to the rapid washout of the radiopharmaceutical from this organ (29). GRPR-targeting radiopharmaceuticals may therefore offer an advantage over [^{177}Lu]Lu-PSMA-617 with respect to safety. The use of GRPR targeting may be of particular importance when radionuclide treatment is considered in earlier stages of PCa, which is currently an active area of research.

Taken together, GRPR-targeting nuclear approaches may complement PSMA targeting in the management of PCa. Therefore, few clinical studies have been initiated making a direct comparison between these two approaches. Since clinical studies are often costly, resource-intensive and time-consuming, investigations are limited to a specific patient population. We believe that preclinical studies can therefore greatly contribute to exploring the potential role of GRPR-targeting applications in the context of the currently applied PSMA targeting for detection and treatment of PCa by studying a broad patient population using the same methodology. To this end, we evaluated and compared *ex vivo* binding of the GRPR- and PSMA-targeting radiopharmaceuticals [^{177}Lu]Lu-NeoB and [^{177}Lu]Lu-PSMA-617, respectively, to patient tissue sections obtained from benign prostatic hyperplasia (BPH), primary PCa and progressive CRPC lesions.

2 Materials and methods

2.1 Human prostate specimens

This study adhered to the Code of Conduct of the Federation of Dutch Medical Scientific Societies. Fresh frozen BPH and primary PCa tissue specimens were retrieved from the Erasmus MC Tissue Bank. BPH tissues (adenomyomatous hyperplasia) from 20 patients (mean age ± standard deviation (SD): 69 ± 10 years) obtained after transurethral resection of the prostate (TURP) and primary PCa tissues from 16 patients (65 ± 7 years) obtained from radical prostatectomy were retrieved. Seventeen CRPC fresh frozen samples were selected from the Erasmus MC Urology Department Tissue Biobank and were obtained from TURP of progressive patients treated in hospitals in the Rotterdam region (73 ± 6 years). Patients were included as CRPC when they presented with biochemical or radiological progressive disease after surgical or medical castration. For the BPH and CRPC sample set, 3 different fragments of one TURP per patient were included to study a larger tissue area. Clinicopathological characteristics, such as Gleason score (GS) and PSA, of all PCa patients are summarized in Tables S1 and S2.

2.2 Tissue sectioning and staining

Each specimen was cut into 10 µm thick sections and mounted on SuperFrost slides (VWR). Adjacent sections were successively used for autoradiography studies with [177Lu]Lu-NeoB (2 sections) and [177Lu]Lu-PSMA-617 (2 sections), 1 section was used for hematoxylin-eosin (H&E) staining, in case of primary PCa 1 section was used for Alpha-methylacyl-CoA racemase (AMACR) staining, and 1 section was used for RNA *in situ* hybridization (ISH) analysis (only in a subset). H&E staining was performed according to a standard protocol in order to determine the presence of cancerous areas. Tumor regions were manually drawn by an experienced pathologist (GvL) and graded according to the ISUP 2014 GS (Table S1). Immunohistochemistry for AMACR was conducted by the Erasmus MC Pathology Research and Trial Service to identify regions of prostatic adenocarcinoma and potentially premalignant high-grade prostatic intraepithelial neoplasia (PIN), although definitive cytological atypia required for the diagnosis of PIN cannot be established well on frozen sections (33). Staining was performed with an automated, validated and accredited staining system (Ventana Benchmark ULTRA, Ventana Medical Systems) using UltraView Universal DAB Detection Kit. In brief, heat-induced antigen retrieval was performed using the Ventana CC1 solution for 8 min. The tissue samples were then incubated with a monoclonal rabbit anti-AMACR (clone 13H4) for 32 min at a concentration of 1.27 µg/mL. Incubation was followed by hematoxylin II counter stain for 12 min and then a blue coloring reagent for 8 min according to the manufactures instructions (Ventana).

High resolution images of the H&E and AMACR stained sections were acquired using a NanoZoomer digital slide scanner (Hamamatsu Photonics) and analyzed using NDP View 2 software (Hamamatsu Photonics).

2.3 Radiopharmaceuticals

The GRPR antagonist NeoB (Advanced Accelerator Applications, a Novartis company) and the PSMA inhibitor PSMA-617 were labeled with lutetium-177 (LuMark, IDB Holland) as described previously (29, 34). Quenchers (ascorbic and gentisic acids) were used to prevent radiolysis (35). High-pressure liquid chromatography and instant thin-layer chromatography on silica gel were used to determine the radiochemical purity (>95%) and radiolabeling yield (>95%) of all labelings. A molar activity of 40 MBq/nmol was used for all *in vitro* autoradiography experiments.

2.4 *In vitro* autoradiography

To compare radiopharmaceutical binding, an *in vitro* autoradiography was performed on frozen human prostate sections. Frozen sections of cell line-derived PC-3 (GRPR-positive) and patient-derived PC295 (PSMA-positive) xenograft tumors were used as positive controls (36, 37). In short, tissue sections were incubated for 10 min at room temperature (RT) with washing buffer (167 mM Tris-HCl pH 7.6, 5 mM MgCl$_2$) containing 0.25% bovine serum albumin (BSA) to prevent non-specific binding to the glass slides. Tissue sections were subsequently incubated for 1 h at RT with 100 µL of incubation buffer (washing buffer with 1% BSA) containing 1 nM [177Lu]Lu-NeoB or [177Lu]Lu-PSMA-617 (i.e. total binding). To assess binding specificity, parallel-sections were co-incubated with an excess (1 µM) of unlabeled Tyr^4-bombesin (Merck Life Science NV) or PSMA-I&T (Huayi Isotopes Co. via ATT Scintomics), respectively. Following incubation, slides were washed and dried before exposure to super-resolution (<50 microns) phosphor screens (Perkin Elmer) for >24 h. Screens were read using the Cyclone (Perkin Elmer) and data was processed in Optiquant software (Perkin Elmer).

[177Lu]Lu-NeoB and [177Lu]Lu-PSMA-617 binding in the tumor regions, as identified on the adjacent H&E-stained sections, was quantified and expressed as digital light units per surface area (DLU/mm^2). Standards consisting of 1 µL drops of incubation buffer were quantified to determine the percentage of added activity per mm^2 (%AA/mm^2). DLU/mm^2 was then converted to %AA/mm^2 by normalizing data to the standards. Specific binding was defined by subtracting the nonspecific binding, as measured on the sections blocked with an excess of unlabeled ligand, from the total binding.

2.5 RNA *in situ* hybridization

RNA ISH assay was performed to determine cellular GRPR and PSMA mRNA expression levels which could be correlated to

radiopharmaceutical binding. To detect GRPR and PSMA mRNA simultaneously in one sample, ISH was performed using the RNAscope 2.5 HD Duplex Reagent Kit (cat. #322430; Advanced Cell Diagnostics (ACD)) in accordance with the manufacturer's instructions for the manual chromogenic assay for fresh frozen tissue using optimized sample preparation and pretreatment conditions. Tissues were fixed in pre-chilled 10% neutral buffered formalin (Sigma-Aldrich) for 2 h at 4°C and then rinsed twice with phosphate buffered saline (PBS; ThermoFisher Scientific). After fixation, tissues were dehydrated using a series of ethanol washes and air dried. For tissue pretreatment, sections were exposed to kit-provided hydrogen peroxide for 10 min at RT and then rinsed in PBS. Immediately after, slides were placed in a dry incubator (37°C) for 30 min before being treated with kit-provided protease IV for 30 min at RT. Hybridization of the GRPR probe Hs-GRPR (cat. #460411; ACD) and the newly designed and synthesized PSMA probe Hs-PSMA1-C2 (cat. #311251-C2; ACD) to target respective mRNA sequences was performed by incubation in the HybEZ Oven (cat. #321720; ACD) for 2 h at 40°C. Hybridization was followed by standard signal amplification steps and fast red and green chromogenic detection. Tissues were then counterstained with Gill's Hematoxylin I (Polysciences Inc.), air dried, mounted and imaged using a NanoZoomer digital slide scanner (Hamamatsu Photonics).

From the whole slide images, regions of interest (ROIs) were selected covering 10% of the tumor area and 5 additional ROIs outside the tumor area to identify non-tumor cell staining. ROIs were manually drawn by a researcher who was blind to the study using QuPath software (38). These ROIs were analyzed using in-house written Python based scripts and graphical interface (Tumor Microenvironment (TME) Analyzer, H.E. Balcioglu, manuscript in preparation), blind to the clinical information (Figure S1). Briefly, the bright field images were converted into pseudo-fluorescent images through image inversion followed by manual identification of signal intensity patterns and using these patterns to assign a pixel intensity per signal (i.e. PSMA probe, GRPR probe and nucleus). To remove nonspecific signal detection, signals low in intensity were removed. Additionally, for the GRPR probe, areas larger than 500px in size were removed to overcome the wrong assignment of brown and blue artifacts to this channel. Nuclei were detected by applying StarDist algorithm '2D_versatile_fluo' (39), and cell regions were assigned through Voronoi segmentation up to 50 pixels from the nucleus. Probe positive regions were detected and clusters were defined as large, elongated regions with at least 100 px^2 size and eccentricity of at least 0.7. Cells were then assigned to 5 bins: bin 0, no probe positivity; bin 1, probe positivity but no clusters; bin 2, 1 probe cluster; bin 3, 2 probe clusters; bin 4, at least 3 probe clusters. H-scores were calculated as follows: H-score = $\sum_{bin}$ (bin number x percentage of cells per bin).
$0 \rightarrow 4$

2.6 Statistics

All statistical analyses were carried out using GraphPad Prism software, version 9 (GraphPad Software Inc.). The distribution of radiopharmaceutical binding within disease stages was depicted in violin plots. When multiple samples from the same patient were available, only one randomly selected sample was used for statistics. As the Shapiro-Wilk test indicated that data was not normally distributed, the nonparametric Kruskal-Wallis test followed by Dunn's *post-hoc* test for multiple comparisons was performed to compare mean GRPR or PSMA radiopharmaceutical binding between disease stages, and between ISUP grades for primary PCa. A *p* value of <0.05 was considered statistically significant. Pearson's correlation coefficient was determined to measure the association between radiopharmaceutical binding and mRNA expression.

3 Results
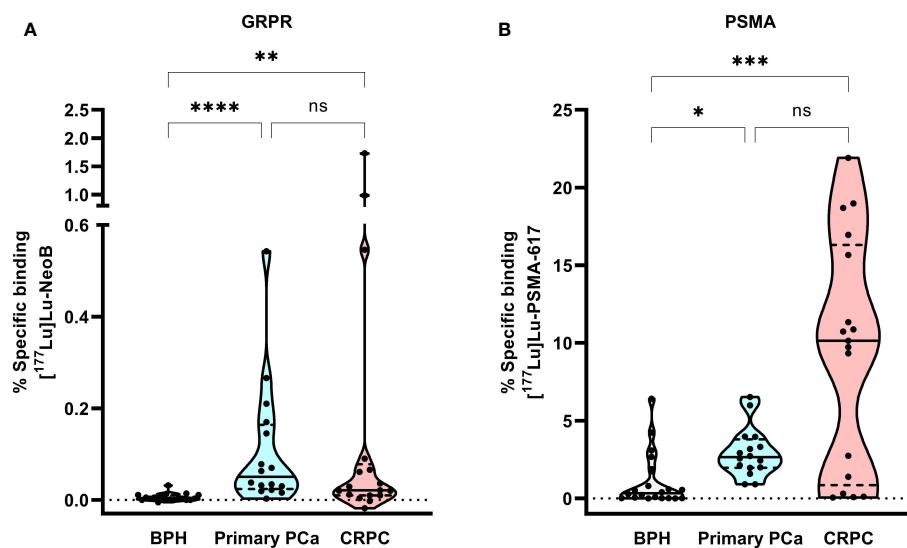
3.1 Binding pattern

Figure 1 shows the percentage specific binding of [177Lu]Lu-NeoB and [177Lu]Lu-PSMA-617 for the individual BPH, primary PCa and CRPC samples. The highest median [177Lu]Lu-NeoB binding (0.051% AA/mm², 95% confidence interval (CI) = 0.034 – 0.183%) was observed in primary PCa samples, while median [177Lu]Lu-PSMA-617 binding (10.74% AA/mm², 95% CI = 5.52 – 13.19%) was highest in CRPC samples. Binding of both radiopharmaceuticals was specific for PCa, as the mean percentage specific binding in both primary PCa and CRPC samples was significantly higher than in BPH (*p* < 0.05). The results of the correlational analysis determined no significant difference in radiopharmaceutical binding by ISUP grade in primary PCa for either [177Lu]Lu-NeoB or [177Lu]Lu-PSMA-617.

The percentage specific binding of [177Lu]Lu-PSMA-617 in 4/20 BPH samples was within or above the upper limit of the 95% CI of binding in primary PCa, indicating relatively high PSMA expression levels in these samples. In contrast, for [177Lu]Lu-NeoB binding this was not true for any of the BPH samples. The highest variation of binding of both radiopharmaceuticals was observed within the CRPC sample set, illustrating that there is a high degree of heterogeneity in GRPR and PSMA expression between patients with advanced disease. Although [177Lu]Lu-PSMA-617 binding was generally high in CRPC samples, 6/17 samples showed no or very low binding (i.e. binding below the lower limit of the 95% CI). Interestingly, one of these samples showed relatively high [177Lu]Lu-NeoB binding. Moreover, 3/17 CRPC samples showed a high level of [177Lu]Lu-NeoB binding that falls outside the 95% probability limit of binding in primary PCa.

3.2 Intrapatient heterogeneity

Next to interpatient heterogeneity, we observed large intrapatient heterogeneity for both [177Lu]Lu-PSMA-617 and [177Lu]Lu-NeoB binding across the various disease states. This intrapatient heterogeneity was reflected in differences in signal intensity between various locations within the prostate and within the tumor region of one section (Figure 2). In order to study the heterogeneity between various locations within the prostate,
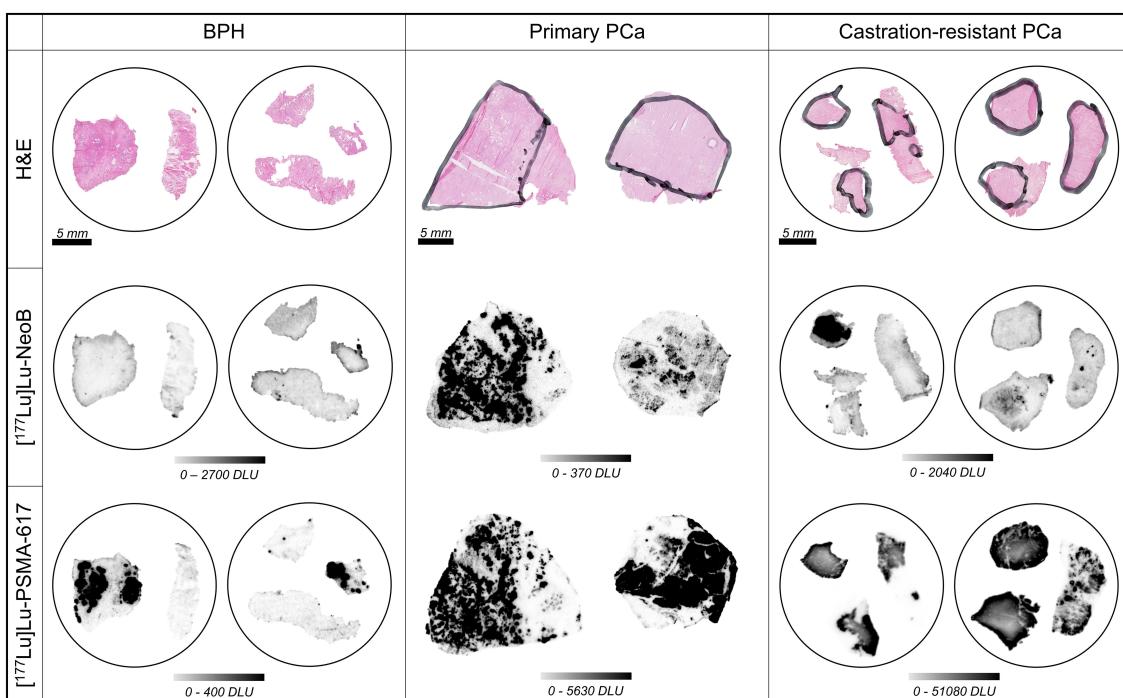
FIGURE 1
Violin plot of the percentage of [^{177}Lu]Lu-NeoB **(A)** and [^{177}Lu]Lu-PSMA-617 **(B)** specific binding to the same set of benign prostatic hyperplasia (BPH; n=20), primary prostate cancer (PCa) (n=16) and castration-resistant PCa (CRPC; n=17) patient samples. The black line represents the median, the dashed lines the two quartiles and the dotted line the 0 axis. Percentage specific binding represents the percentage of added activity per mm^2. * = $p < 0.05$, ** = $p < 0.01$ and **** = $p < 0.0001$, GRPR, gastrin-releasing peptide receptor; ns, not significant; PSMA, prostate-specific membrane antigen.

fragments from different sites in the prostate or prostate tumor of the same patient were analyzed for the BPH and CRPC stages, respectively. It was observed that not all samples from the same patient showed binding or showed the same degree of binding.

3.3 Tumor specificity

Analysis of tumor specificity was conducted in the relatively larger sections of the primary PCa samples using H&E and AMACR

FIGURE 2
Hematoxylin-eosin (H&E) stains (top row), binding of [^{177}Lu]Lu-NeoB (middle row) and [^{177}Lu]Lu-PSMA-617 (bottom row) to representative samples of benign prostatic hyperplasia (BPH), primary prostate cancer (PCa) and castration-resistant PCa. Encircled tissue sections belong to the same patient. The black marking in the H&E stained sections indicates tumor area(s) as identified by a pathologist. The scale selected for the autoradiography sections shows optimized contrast. DLU, digital light unit.

stainings to detect prostatic adenocarcinoma cells. This analysis showed that binding of [^{177}Lu]Lu-PSMA-617 and [^{177}Lu]Lu-NeoB occurred in a focal pattern that corresponded with AMACR staining intensity (Figure 3). Small areas of AMACR positively stained cells were observed within and outside the tumor regions identified by H&E supported pathology. In the majority of cases, these AMACR positive areas outside of the tumor region also showed relatively high [^{177}Lu]Lu-PSMA-617 and [^{177}Lu]Lu-NeoB binding and may represent premalignant high-grade PIN. Interestingly, in 5/16 cases (3/5 ISUP grade 2, 2/5 ISUP grade 3) high [^{177}Lu]Lu-PSMA-617 binding and in contrast no or very little [^{177}Lu]Lu-NeoB binding was observed to cells outside the tumor region and AMACR positively stained areas (i.e. normal tissue). Here, histological evaluation revealed the presence of normal epithelial cells lining glandular ducts. The high [^{177}Lu]Lu-PSMA-617 binding was target specific as no binding was observed in the blocked section (Figure S2).

3.4 mRNA expression

An RNA ISH assay was conducted to evaluate the relation between mRNA expression and radiopharmaceutical binding (Figure 4, Figure S3). Although significance was not observed, probably due to the low number of samples, PSMA mRNA expression levels (expressed as H-score) showed a trend that correlated positively with radiopharmaceutical binding ($n = 5$; $r = 0.64$; $p = 0.25$). No strong trend was found for GRPR ($n = 5$; $r = 0.34$; $p = 0.57$). In line with the results of the autoradiography studies, the H-score for PSMA was significantly higher than for GRPR (mean ± SD; 72.4 ± 18.1 for PSMA vs. 10.0 ± 5.4 for GRPR; $p < 0.01$),

indicating higher PSMA expression (Table S3). PSMA mRNA levels in non-tumor areas were also significantly higher than GRPR mRNA levels ($p < 0.05$) (Table S4). Moreover, analysis showed that of all target-positive cells there was a considerable proportion of single positive cells (range; 76.7-92.8% and 12.4-43.9% for PSMA and GRPR positive cells, respectively), reflecting the distinct expression patterns of PSMA and GRPR.

4 Discussion

PSMA-targeting radiopharmaceuticals have emerged as powerful agents for PCa management. However, not all PCa patients have PSMA overexpression and a considerable proportion of PSMA-positive patients does not respond to treatment with [^{177}Lu]Lu-PSMA-617. Moreover, PSMA targeting comes with serious side effects as the result of unwanted but specific binding to PSMA on the salivary glands. This calls for improved PCa theranostics by, for example, using other targets. In this study, we examined whether GRPR-targeting radiopharmaceuticals can complement PSMA-targeting theranostic approaches and where to position them in the progression of PCa. We compared [^{177}Lu]Lu-NeoB and [^{177}Lu]Lu-PSMA-617 binding in patient samples of BPH, primary PCa and CRPC using the same methodology across all stages. Whilst some clinical research has been carried out on such a comparison, in this preclinical research we were able to cover a broad range of prostate conditions thereby our study contributes to an increased understanding of the link between radiopharmaceutical binding and disease stage.

The data showed the highest median binding of [^{177}Lu]Lu-NeoB in primary PCa samples, while the highest median binding of
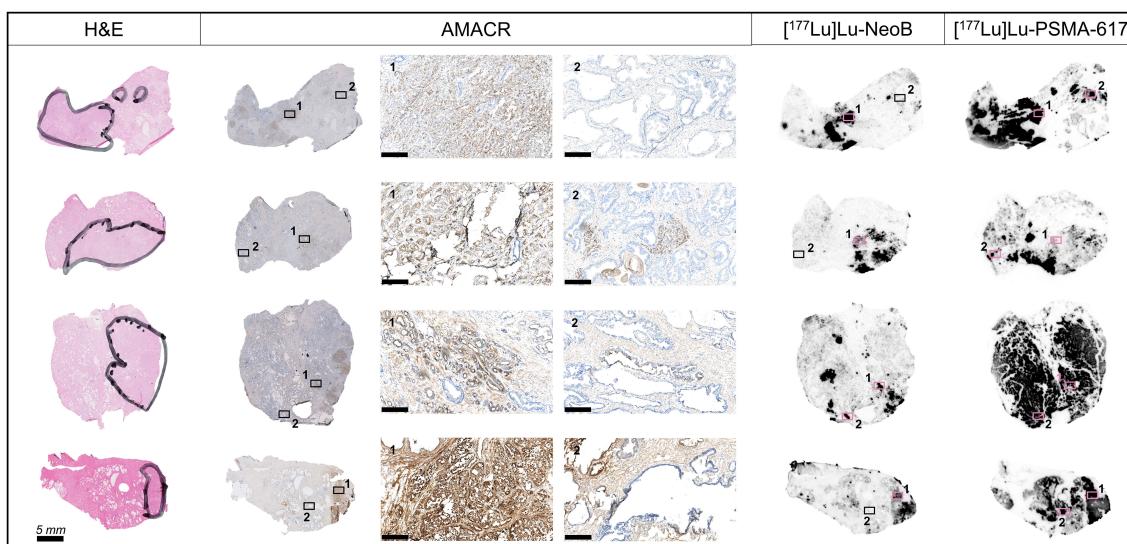
FIGURE 3
Tumor specificity of [^{177}Lu]Lu-NeoB and [^{177}Lu]Lu-PSMA-617 in primary prostate cancer sections of four representative patients. From left to right in the figure: hematoxylin-eosin (H&E) staining, immunohistochemical staining of alpha-methylacyl-CoA racemase (AMACR) expression, [^{177}Lu]Lu-NeoB and [^{177}Lu]Lu-PSMA-617 binding. The black marking in the H&E stained sections indicates the tumor area(s) as identified by a pathologist. For the AMACR stained section, a 10x magnification of two specified areas (black/pink box numbered 1 or 2) is shown (scale bar = 250 μm). The presented autoradiography sections are displayed at an optimal scale for each tissue to show optimized contrast.
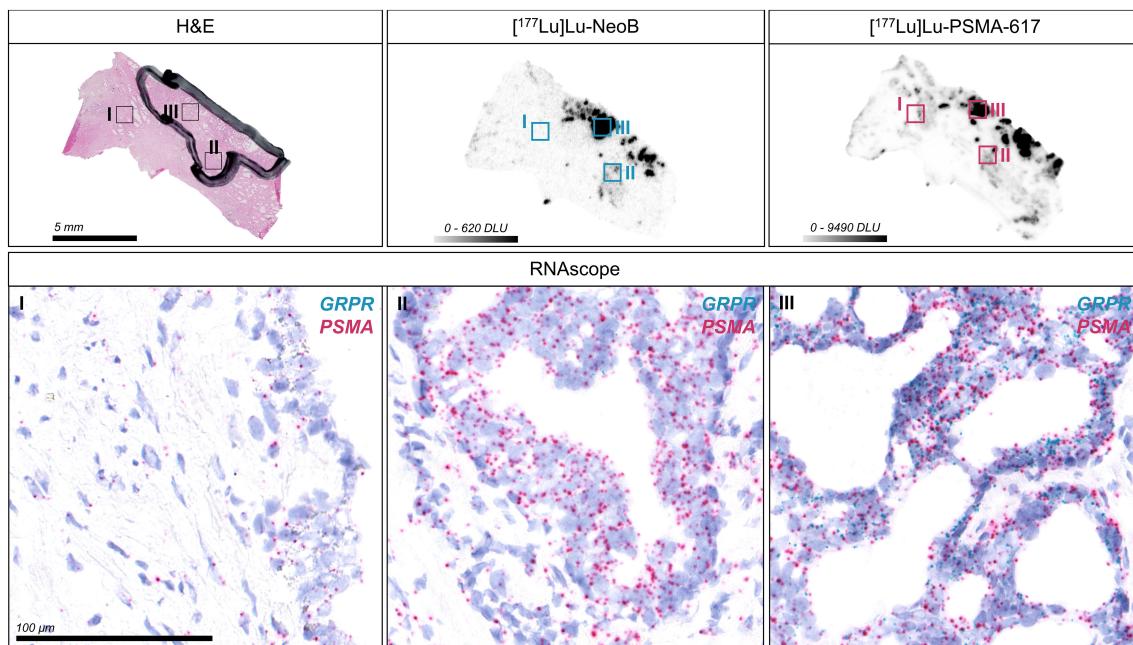
FIGURE 4

Detection of gastrin-releasing peptide receptor (GRPR) and prostate-specific membrane antigen (PSMA) mRNA expression in one representative primary prostate cancer section using RNA *in situ* hybridization (ISH). The hematoxylin-eosin (H&E) stained section with black marking indicates the tumor area as identified by a pathologist. The corresponding autoradiography images for [177Lu]Lu-NeoB and [177Lu]Lu-PSMA-617 binding are displayed and the selected color scale shows the optimized contrast for the sections. Forty times magnifications of the RNA ISH section showing a region with background [177Lu]Lu-NeoB and [177Lu]Lu-PSMA-617 binding in non-tumor tissue (I) and with relatively low (II) and high (III) binding within the tumor are shown. Each dot represents a single GRPR (blue) or PSMA (red) mRNA molecule. Nuclei were counterstained with hematoxylin (purple). DLU, digital light unit.

[177Lu]Lu-PSMA-617 was observed in CRPC samples. This finding confirms the work of others, in which high GRPR and PSMA expression were linked to the respective disease stages (5, 18). Although, in contrast to our previous report on breast cancer (40), we did not observe a statistically significant relationship between radiopharmaceutical binding and target mRNA expression, we expect this to be due to sample size rather than different tissue type. Even though we found the highest median binding of [177Lu]Lu-NeoB in primary PCa, the 3 samples with the highest [177Lu]Lu-NeoB binding belonged to the CRPC sample set. This may suggest that GRPR-targeting approaches may be relevant in a small proportion of patients with late stage disease.

We observed that 1/6 PSMA-negative CRPC samples showed high [177Lu]Lu-NeoB binding, indicating a potential complementary role of GRPR targeting to PSMA theranostics. Although these are low numbers, Baratto et al. (41) also underlined the complementary value of GRPR targeting as they identified 7 additional lesions with [68Ga]Ga-RM2 (a potent GRPR-targeting agent) PET that were not visible on [68Ga]Ga-PSMA11/ [18F]F-DCFPyL PET in 4/50 biochemically recurrent PCa patients. Kurth et al. (28) investigated 35 patients with metastatic CRPC who had insufficient PSMA expression or showed lower tumor accumulation after previous cycles of [177Lu]Lu-PSMA-617 treatment. They identified 6 patients with high uptake on [68Ga]

Ga-RM2 PET/CT and who thus qualified for [177Lu]Lu-RM2 therapy. In their study, the absorbed doses in the tumor lesions delivered by [177Lu]Lu-RM2 were found to be therapeutically relevant. Taken together, our findings support that a subset of metastatic CRPC patients might benefit from GRPR-mediated radionuclide therapy.

Although [177Lu]Lu-PSMA-617 radionuclide therapy is currently only available for patients with metastatic CRPC, further studies are ongoing to explore its use in earlier stages of PCa. In our study, we observed binding of both [177Lu]Lu-NeoB and [177Lu]Lu-PSMA-617 in all but one primary PCa samples. This finding is consistent with that of Mapelli et al. (42) who reported detection of primary PCa in 18/19 patients with both GRPR- and PSMA-targeting radiopharmaceuticals separately. A limitation for the use of PSMA radiopharmaceuticals in primary PCa is the relatively high binding of [177Lu]Lu-PSMA-617 to BPH samples and normal tissue surrounding primary PCa with ISUP grade 2 and 3, as observed in our study. Our results indicate that PSMA-targeting applications, in contrast to GRPR, may not always distinguish cancerous tissue from benign or normal tissue, reducing the tumor-specific value. This is one of the pitfalls of PSMA PET that has also been described before (43).

Analyzing radiopharmaceutical binding in primary PCa within the ISUP grades for PCa classification revealed no significant

differences between grades. However, prior preclinical studies evaluating the expression of GRPR and PSMA in PCa samples have reported on a higher GRPR expression for low-grade PCa specimens. Faviana et al. (44) found that the number of cells expressing GRPR as determined by immunohistochemistry was significantly higher in low-grade tumors and Schollhammer et al. (45) demonstrated higher $[^{111}In]$In-RM2 binding in primary PCa samples with Gleason score 6 (i.e. ISUP grade 1) using autoradiography studies. The absence of a found correlation in our study may be due to the unequal distribution of samples across the 5 ISUP grade groups in combination with the small sample size reducing the statistical power. Unlike the aforementioned studies, our primary objective was to compare expression levels across the different disease stages and thus ISUP grade was not taken into account when samples were selected. Similarly as our study contrasts with other preclinical reports, clinical studies reported contradictory results as well; Gao et al. (46) noted higher uptake in low-ISUP PCa, while Schollhammer et al. (47) saw no differences in uptake between ISUP grades for GRPR-mediated PET/CT. More research is needed to get a clear answer on the association between ISUP grade and GRPR expression levels in primary PCa.

For primary PCa, the complementary value of GRPR targeting may also be found in the fact that we observed binding of $[^{177}Lu]$Lu-NeoB and $[^{177}Lu]$Lu-PSMA-617 to overlapping, but also to different tumor areas within the tumor region of one sample. This finding of distinct GRPR and PSMA expression patterns was further supported by our RNA ISH results indicating differential mRNA expression of these targets per cell. There was a considerable proportion of single positive cells that showed mRNA signal only for GRPR or PSMA, although GRPR positivity might be underestimated due to color overlap with the cell nucleus. This complementary role for GRPR-targeting radiopharmaceuticals based on the different expression patterns has also been suggested in previous studies (48, 49). The observed intrapatient heterogeneity of GRPR and PSMA suggests that future theranostics for primary prostate tumors may benefit from an approach in which GRPR- and PSMA-targeting radiopharmaceuticals are combined. One such approach currently being explored by various research groups is the use of GRPR/PSMA-targeting heterodimers (50–52). Reported results so far are preliminary and the value of such heterodimers remains to be investigated. Of note, if GRPR/PSMA heterodimers will be applied for radionuclide therapy, the off-target organ toxicity should critically be evaluated as GRPR and PSMA are physiologically expressed on different background organs, which may increase toxicity.

The generalizability of these results is subject to limitations. While autoradiography studies provide a direct measurement of radiopharmaceutical binding and allow for the high-resolution visualization of binding, this does not reflect *in vivo* pharmacokinetics. The large difference in specific binding of $[^{177}Lu]$Lu-NeoB and $[^{177}Lu]$Lu-PSMA-617 observed in our study could partly be attributed to this, as the difference in SUVmax in PET studies is generally much smaller. Furthermore, because of the heterogeneous CRPC sample set, correlations with clinicopathological parameters were not addressed in this study. With regard to the RNA ISH analysis, only a single primary PCa section was analyzed per patient

for a limited number of patients, limiting the statistical significance of our findings. Therefore, given the general knowledge of tumor heterogeneity, we should interpret our results with caution. Despite these limitations, our study contributes to the knowledge of GRPR and PSMA expression profiles across PCa disease stages and their use as potential targets for theranostic applications.

5 Conclusion

Our study demonstrates that GRPR-targeting radiopharmaceuticals may have complementary value for a theranostic approach in both early and late stages of PCa. Furthermore, we showed that relatively high PSMA binding, in contrast to GRPR binding, may be non-tumor specific at early stage PCa. Our study contributes to a better understanding of how to position GRPR targeting in the context of PSMA-directed PCa theranostics to ultimately advance clinical care for PCa patients.

Data availability statement

The original contributions presented in the study are included in the article/Supplementary Material. Further inquiries can be directed to the corresponding author.

Ethics statement

Ethical review and approval was not required for the study on tissue specimens of human participants in accordance with the local legislation and institutional requirements. The patients/participants provided their written informed consent to participate in this study.

Author contributions

Conceptualization: SD. Design: WW and SD. Data acquisition: MV, ER and LB. Data analysis: MV, ER, GL, LB and HB. Data interpretation: MV, ER, WW and SD. Writing the first draft of the manuscript: MV. Critically reviewing the manuscript: ER, GL, HB, WW and SD. All authors read and approved the submitted version.

Funding

Acknowledgments

Conflict of interest

The authors declare that the research was conducted in the absence of any commercial or financial relationships that could be construed as a potential conflict of interest.

Publisher's note

All claims expressed in this article are solely those of the authors and do not necessarily represent those of their affiliated organizations, or those of the publisher, the editors and the reviewers. Any product that may be evaluated in this article, or claim that may be made by its manufacturer, is not guaranteed or endorsed by the publisher.

Supplementary material

The Supplementary Material for this article can be found online at: https://www.frontiersin.org/articles/10.3389/fonc.2023.1199432/full#supplementary-material

References

1. Sung H, Ferlay J, Siegel RL, Laversanne M, Soerjomataram I, Jemal A, et al. Global Cancer Statistics 2020: GLOBOCAN estimates of incidence and mortality worldwide for 36 cancers in 185 countries. *CA: A Cancer J Clin* (2021) 71(3):209–49. doi: 10.3322/caac.21660

2. O'Dwyer E, Bodei L, Morris MJ. The role of theranostics in prostate cancer. *Semin Radiat Oncol* (2021) 31(1):71–82. doi: 10.1016/j.semradonc.2020.07.004

3. Silver DA, Pellicer I, Fair WR, Heston WD, Cordon-Cardo C. Prostate-specific membrane antigen expression in normal and Malignant human tissues. *Clin Cancer Res* (1997) 3(1):81–5.

4. Sweat SD, Pacelli A, Murphy GP, Bostwick DG. Prostate-specific membrane antigen expression is greatest in prostate adenocarcinoma and lymph node metastases. *Urology* (1998) 52(4):637–40. doi: 10.1016/S0090-4295(98)00278-7

5. Wright GL Jr., Haley C, Beckett ML, Schellhammer PF. Expression of prostate-specific membrane antigen in normal, benign, and Malignant prostate tissues. *Urol Oncol* (1995) 1(1):18–28. doi: 10.1016/1078-1439(95)00002-Y

6. Bostwick DG, Pacelli A, Blute M, Roche P, Murphy GP. Prostate specific membrane antigen expression in prostatic intraepithelial neoplasia and adenocarcinoma. *Cancer* (1998) 82(11):2256–61. doi: 10.1002/(SICI)1097-0142(19980601)82:11<2256::AID-CNCR22>3.0.CO;2-S

7. FDA approves first PSMA-targeted PET drug. *J Nucl Med* (2021) 62(2):11N–N.

8. FDA approves ^{18}F-DCFPyL PET agent in prostate cancer. *J Nucl Med* (2021) 62(8):11N–N.

9. FDA approves pluvicto/locametz for metastatic castration-resistant prostate cancer. *J Nucl Med* (2022) 63(5):13N–N.

10. Perera M, Papa N, Christidis D, Wetherell D, Hofman MS, Murphy DG, et al. Sensitivity, specificity, and predictors of positive 68Ga–prostate-specific membrane antigen positron emission tomography in advanced prostate cancer: A systematic review and meta-analysis. *Eur Urology*. (2016) 70(6):926–37. doi: 10.1016/j.eururo.2016.06.021

11. Sonni I, Eiber M, Fendler WP, Alano RM, Vangala SS, Kishan AU, et al. Impact of ^{68}Ga-PSMA-11 PET/CT on staging and management of prostate cancer patients in various clinical settings: A prospective single-center study. *J Nucl Med* (2020) 61(8):1153–60. doi: 10.2967/jnumed.119.237602

12. Sartor O, de Bono J, Chi KN, Fizazi K, Herrmann K, Rahbar K, et al. Lutetium-177-PSMA-617 for metastatic castration-resistant prostate cancer. *N Engl J Med* (2021) 385(12):1091–103. doi: 10.1056/NEJMoa2107322

13. Sadaghiani MS, Sheikhbahaei S, Werner RA, Pienta KJ, Pomper MG, Solnes LB, et al. A systematic review and meta-analysis of the effectiveness and toxicities of lutetium-177–labeled prostate-specific membrane antigen–targeted radioligand therapy in metastatic castration-resistant prostate cancer. *Eur Urology*. (2021) 80 (1):82–94. doi: 10.1016/j.eururo.2021.03.004

14. Michael SH, Rodney JH, Tobias M, Matthias E. Prostate-specific membrane antigen PET: clinical utility in prostate cancer, normal patterns, pearls, and pitfalls. *RadioGraphics* (2018) 38(1):200–17. doi: 10.1148/rg.2018170108

15. Ling SW, de Blois E, Hooijman E, van der Veldt A, Brabander T. Advances in 177Lu-PSMA and 225Ac-PSMA radionuclide therapy for metastatic castration-resistant prostate cancer. *Pharmaceutics* (2022) 14(10):2166. doi: 10.3390/pharmaceutics14102166

16. Baratto L, Duan H, Mäcke H, Iagaru A. Imaging the distribution of gastrin-releasing peptide receptors in cancer. *J Nucl Med* (2020) 61(6):792–8. doi: 10.2967/jnumed.119.234971

17. Cornelio DB, Roesler R, Schwartsmann G. Gastrin-releasing peptide receptor as a molecular target in experimental anticancer therapy. *Ann Oncol* (2007) 18(9):1457–66. doi: 10.1093/annonc/mdm058

18. Beer M, Montani M, Gerhardt J, Wild PJ, Hany TF, Hermanns T, et al. Profiling gastrin-releasing peptide receptor in prostate tissues: Clinical implications and molecular correlates. *Prostate.* (2012) 72(3):318–25. doi: 10.1002/pros.21434

19. Markwalder R, Reubi JC. Gastrin-releasing peptide receptors in the human prostate: relation to neoplastic transformation. *Cancer Res* (1999) 59(5):1152–9.

20. Reubi JC, Wenger S, Schmuckli-Maurer J, Schaer J-C, Gugger M. Bombesin receptor subtypes in human cancers: detection with the universal radioligand 125I-[D-TYR6, β-ALA11, PHE13, NLE14] bombesin (6–14). *Clin Cancer Res* (2002) 8(4):1139–46.

21. Bartholdi MF, Wu JM, Pu H, Troncoso P, Eden PA, Feldman RI. In situ hybridization for gastrin-releasing peptide receptor (GRP receptor) expression in prostatic carcinoma. *Int J cancer.* (1998) 79(1):82–90. doi: 10.1002/(SICI)1097-0215(19980220)79:1<82::AID-IJC16>3.0.CO;2-J

22. Sun B, Halmos G, Schally AV, Wang X, Martinez M. Presence of receptors for bombesin/gastrin-releasing peptide and mRNA for three receptor subtypes in human prostate cancers. *Prostate.* (2000) 42(4):295–303. doi: 10.1002/(SICI)1097-0045(20000301)42:4<295::AID-PROS7>3.0.CO;2-B

23. Minamimoto R, Sonni I, Hancock S, Vasanawala S, Loening A, Gambhir SS, et al. Prospective evaluation of (68)Ga-RM2 PET/MRI in patients with biochemical recurrence of prostate cancer and negative findings on conventional imaging. *J Nucl Med* (2018) 59(5):803–8. doi: 10.2967/jnumed.117.197624

24. Wieser G, Popp I, Christian Rischke H, Drendel V, Grosu AL, Bartholomä M, et al. Diagnosis of recurrent prostate cancer with PET/CT imaging using the gastrin-releasing peptide receptor antagonist (68)Ga-RM2: Preliminary results in patients with negative or inconclusive [(18)F]Fluoroethylcholine-PET/CT. *Eur J Nucl Med Mol Imaging.* (2017) 44(9):1463–72. doi: 10.1007/s00259-017-3702-8

25. Bakker IL, Fröberg AC, Busstra MB, Verzijlbergen JF, Konijnenberg M, van Leenders G, et al. GRPr antagonist (68)Ga-SB3 PET/CT imaging of primary prostate cancer in therapy-naïve patients. *J Nucl Med* (2021) 62(11):1517–23. doi: 10.2967/jnumed.120.258814

26. Zhang J, Niu G, Fan X, Lang L, Hou G, Chen L, et al. PET using a GRPR antagonist (68)Ga-RM26 in healthy volunteers and prostate cancer patients. *J Nucl Med* (2018) 59(6):922–8. doi: 10.2967/jnumed.117.198929

27. Nock BA, Kaloudi A, Lymperis E, Giarika A, Kulkarni HR, Klette I, et al. Theranostic perspectives in prostate cancer with the gastrin-releasing peptide receptor antagonist neoBOMB1: preclinical and first clinical results. *J Nucl Med* (2017) 58 (1):75–80. doi: 10.2967/jnumed.116.178889

28. Kurth J, Krause BJ, Schwarzenböck SM, Bergner C, Hakenberg OW, Heuschkel M. First-in-human dosimetry of gastrin-releasing peptide receptor antagonist [177Lu] Lu-RM2: a radiopharmaceutical for the treatment of metastatic castration-resistant prostate cancer. *Eur J Nucl Med Mol Imaging.* (2020) 47(1):123–35. doi: 10.1007/s00259-019-04504-3

29. Dalm SU, Bakker IL, de Blois E, Doeswijk GN, Konijnenberg MW, Orlandi F, et al. 68Ga/177Lu-neoBOMB1, a novel radiolabeled GRPR antagonist for theranostic use in oncology. *J Nucl Med* (2017) 58(2):293–9. doi: 10.2967/jnumed.116.176636

30. Montemagno C, Raes F, Ahmadi M, Bacot S, Debiossat M, Leenhardt J, et al. In vivo biodistribution and efficacy evaluation of neoB, a radiotracer targeted to GRPR, in mice bearing gastrointestinal stromal tumor. *Cancers (Basel)* (2021) 13(5):1051. doi: 10.3390/cancers13051051

31. Gruber L, Decristoforo C, Uprimny C, Hohenberger P, Schoenberg SO, Orlandi F, et al. Imaging properties and tumor targeting of 68Ga-neoBOMB1, a gastrin-releasing peptide receptor antagonist, in GIST patients. *Biomedicines* (2022) 10 (11):2899. doi: 10.3390/biomedicines10112899

32. Ruigrok EAM, Verhoeven M, Konijnenberg MW, de Blois E, de Ridder CMA, Stuurman DC, et al. Safety of [177Lu]Lu-NeoB treatment: a preclinical study

characterizing absorbed dose and acute, early, and late organ toxicity. *Eur J Nucl Med Mol Imaging* (2022) 49(13):4440–4451. doi: 10.1007/s00259-022-05926-2

33. Jiang Z, Woda BA, Wu C-L, Yang XJ. Discovery and clinical application of a novel prostate cancer marker: α-methylacyl CoA racemase (P504S). *Am J Clin Pathology*. (2004) 122(2):275–89. doi: 10.1309/EJUYUQPEX1MG68MK

34. de Zanger RMS, Chan HS, Breeman WAP, de Blois E. Maintaining radiochemical purity of [177Lu]Lu-DOTA-PSMA-617 for PRRT by reducing radiolysis. *J Radioanalytical Nucl Chem* (2019) 321(1):285–91. doi: 10.1007/s10967-019-06573-y

35. de Blois E, Sze Chan H, Konijnenberg M, de Zanger R, A.P. Breeman W. Effectiveness of quenchers to reduce radiolysis of 111In- or 177Lu-labelled methionine-containing regulatory peptides. Maintaining radiochemical purity as measured by HPLC. *Curr Topics Medicinal Chem* (2012) 12(23):2677–85. doi: 10.2174/1568026611212230005

36. Reile H, Armatis PE, Schally AV. Characterization of high-affinity receptors for bombesin/gastrin releasing peptide on the human prostate cancer cell lines PC-3 and DU-145: Internalization of receptor bound 125I-(Tyr4) bombesin by tumor cells. *Prostate*. (1994) 25(1):29–38. doi: 10.1002/pros.2990250105

37. van Weerden WM, de Ridder CM, Verdaasdonk CL, Romijn JC, van der Kwast TH, Schröder FH, et al. Development of seven new human prostate tumor xenograft models and their histopathological characterization. *Am J Pathol* (1996) 149(3):1055–62.

38. Bankhead P, Loughrey MB, Fernández JA, Dombrowski Y, McArt DG, Dunne PD, et al. QuPath: Open source software for digital pathology image analysis. *Sci Rep* (2017) 7(1):16878. doi: 10.1038/s41598-017-17204-5

39. Schmidt U, Weigert M, Broaddus C, Myers G. *Cell Detection with Star-Convex Polygons. Medical Image Computing and Computer Assisted Intervention – MICCAI 2018*. Cham: Springer International Publishing (2018).

40. Dalm SU, Sieuwerts AM, Look MP, Melis M, van Deurzen CH, Foekens JA, et al. Clinical relevance of targeting the gastrin-releasing peptide receptor, somatostatin receptor 2, or chemokine C-X-C motif receptor 4 in breast cancer for imaging and therapy. *J Nucl Med* (2015) 56(10):1487–93. doi: 10.2967/jnumed.115.160739

41. Baratto L, Song H, Duan H, Hatami N, Bagshaw HP, Buyyounouski M, et al. PSMA- and GRPR-targeted PET: results from 50 patients with biochemically recurrent prostate cancer. *J Nucl Med* (2021) 62(11):1545–9. doi: 10.2967/jnumed.120.259630

42. Mapelli P, Ghezzo S, Samanes Gajate AM, Preza E, Brembilla G, Cucchiara V, et al. Preliminary results of an ongoing prospective clinical trial on the use of (68)Ga-PSMA and (68)Ga-DOTA-RM2 PET/MRI in staging of high-risk prostate cancer patients. *Diagnostics (Basel)* (2021) 11(11):2068. doi: 10.3390/diagnostics11112068

43. Shetty D, Patel D, Le K, Bui C, Mansberg R. Pitfalls in gallium-68 PSMA PET/CT interpretation-A pictorial review. *Tomography* (2018) 4(4):182–93. doi: 10.18383/j.tom.2018.00021

44. Faviana P, Boldrini L, Erba PA, Di Stefano I, Manassero F, Bartoletti R, et al. Gastrin-releasing peptide receptor in low grade prostate cancer: can it be a better predictor than prostate-specific membrane antigen? *Front Oncol* (2021) 11:650249. doi: 10.3389/fonc.2021.650249

45. Schollhammer R, De Clermont Gallerande H, Yacoub M, Quintyn Ranty ML, Barthe N, Vimont D, et al. Comparison of the radiolabeled PSMA-inhibitor (111)In-PSMA-617 and the radiolabeled GRP-R antagonist (111)In-RM2 in primary prostate cancer samples. *EJNMMI Res* (2019) 9(1):52. doi: 10.1186/s13550-019-0517-6

46. Gao X, Tang Y, Chen M, Li J, Yin H, Gan Y, et al. A prospective comparative study of [(68)Ga]Ga-RM26 and [(68)Ga]Ga-PSMA-617 PET/CT imaging in suspicious prostate cancer. *Eur J Nucl Med Mol Imaging* (2023) 50(7):2177–2187. doi: 10.21203/rs.3.rs-2175723/v1

47. Schollhammer R, Robert G, Asselineau J, Yacoub M, Vimont D, Balamoutoff N, et al. Comparison of 68Ga-PSMA-617 PET/CT and 68Ga-RM2 PET/CT in patients with localized prostate cancer who are candidates for radical prostatectomy: A prospective, single-arm, single-center, phase II study. *J Nucl Med* (2023) 64(3):379–85. doi: 10.2967/jnumed.122.263889

48. Duan H, Baratto L, Fan RE, Soerensen SJC, Liang T, Chung BI, et al. Correlation of (68)Ga-RM2 PET with post-surgery histopathology findings in patients with newly diagnosed intermediate- or high-risk prostate cancer. *J Nucl Med* (2022) 63(12):1829–1835. doi: 10.2967/jnumed.122.263971

49. Fassbender TF, Schiller F, Zamboglou C, Drendel V, Kiefer S, Jilg CA, et al. Voxel-based comparison of [68Ga]Ga-RM2-PET/CT and [68Ga]Ga-PSMA-11-PET/CT with histopathology for diagnosis of primary prostate cancer. *EJNMMI Res* (2020) 10(1):62. doi: 10.1186/s13550-020-00652-y

50. Eder M, Schäfer M, Bauder-Wüst U, Haberkorn U, Eisenhut M, Kopka K. Preclinical evaluation of a bispecific low-molecular heterodimer targeting both PSMA and GRPN for improved PET imaging and therapy of prostate cancer. *Prostate*. (2014) 74(6):659–68. doi: 10.1002/pros.22784

51. Mitran B, Varasteh Z, Abouzayed A, Rinne SS, Puuvuori E, De Rosa M, et al. Bispecific GRPR-antagonistic anti-PSMA/GRPR heterodimer for PET and SPECT diagnostic imaging of prostate cancer. *Cancers* (2019) 11(9):1371. doi: 10.3390/cancers11091371

52. Lundmark F, Abouzayed A, Rinne SS, Timofeev V, Sipkina N, Naan M, et al. Preclinical characterisation of PSMA/GRPR-targeting heterodimer [68Ga]Ga-BQ7812 for PET diagnostic imaging of prostate cancer: A step towards clinical translation. *Cancers* (2023) 15(2):442. doi: 10.3390/cancers15020442